Direct laser writing of optical gratings on additive manufactured metal surfaces

Ruck, Simon; Kleefoot, Max-Jonathan; Harrison, David K.; De Silva, Anjali; Riegel, Harald

Published in:
Procedia CIRP

DOI:
10.1016/j.procir.2022.08.004

Publication date:
2022

Document Version
Publisher's PDF, also known as Version of record

Available online at www.sciencedirect.com

ScienceDirect

Procedia CIRP 111 (2022) 653–656

www.elsevier.com/locate/procedia

12th CIRP Conference on Photonic Technologies [LANE 2022], 4-8 September 2022, Fürth, Germany

Direct laser writing of optical gratings on additive manufactured metal surfaces

Simon Ruck[a,b,*], Max-Jonathan Kleefoot[a], David K Harrison[b], Anjali De Silva[b], Harald Riegel[a]

[a]*LaserApplikationsZentrum, Aalen University, Beethovenstr.1, 73430 Aalen, Germany*
[b] *School of Computing, Engineering & Built Environment, Glasgow Caledonian University, Cowcaddens Road, Glasgow, G4 0BA, Scotland, UK*

* Corresponding author. Tel.: +49 7361 576-2728. *E-mail address:* simon.ruck@hs-aalen.de

Abstract

Enhancing the functionality of surfaces has increasingly become the focus of modern engineering in recent years. Functional material surfaces can be developed through targeted micro structuring. For example, surface modifications by micro structuring can change the wetting behaviour or effectively optimize the frictional properties. Some of these applications are already established on the market and e.g. used in case of improving highly stressed surfaces. To accelerate further research in this direction, the present work deals with the functionalization of surfaces with the aim of modifying optical properties. The overall vision for this is the production of functional enhanced additive manufactured free-form mirrors for technical applications. Nowadays, the additive manufactured metal mirrors need a complicated and time-consuming mechanical post-processing like e.g. manual polishing. To add a further functionalization, structures like e.g. optical gratings need a separate production step, mostly limited to one fix structure geometry and size. Thus, laser direct writing as an alternative method and highly flexible production process is examined.

Keywords: ultra-short pulsed laser ablation, post-processing additive manufacturing, metal optics, surface processing

1. Introduction

During the last decade, Additive Manufacturing (AM), also called 3D printing, has become game changing manufacturing technology, which allows the production of highly complex parts. Today, AM is not only a technology used for the developing of new parts and prototypes, it is also an important technology for serial production. Examples for real and end-use parts can be found in a wide range of various industrial applications [1].

The key principle of this technology is adding material to a volume, mostly done by printing layer by layer, only where it is needed. Depending on the used printing machine, nearly all geometries are able to be produced and therefore a big economic impact is expected [2]. Since the initial materials such as metal powders or polymers are expensive to procure, AM should only be used if added value can be created or the desired part cannot be manufactured in any other way.

An interesting application area where AM can be an optimal solution for the production of special parts is the printing of complex optical freeform elements. To date, there have been comparatively few successful research activities in this field, as high demands are placed on the optical properties of the end components for real applications [3]. Mostly, polymer or polymer-glass suspensions are processes using two-photon polymerization, stereo lithography or inkjet based printing systems, aiming to build new transmitting optics [4, 5]. However, the layer-wise build process causes some disadvantages in the use of this optics for light transmission, e.g. absorption and scattering at the interface of the single layers [3]. This leads to a limited transmission value and a limited damage threshold, especially for polymer optics in the lower field of visible light radiation. As example [3] reached a

10.1016/j.procir.2022.08.004

transitivity of 70% to max. 95% at a wavelength of 500 nm, strongly dependant on the used material. Thus, another approach has to be pursued for additive manufactured optics considering high power or low wavelength applications. Therefore, a possible solution is AM of reflective metal optics, e.g. made of aluminum or aluminum alloys [6, 7]. Aluminum and aluminum alloys have proven a high reflectivity for a broad band of wavelengths [8, 9]. In addition, these materials exhibit a high thermal conductivity, which is positive if also inner cooling is whished. At least, they are cheap in production and well processable compared to other high reflective materials such as copper. However, also for additive manufactured reflective optics the surface roughness and waviness due to the layer-wise AM process are a big issue [6]. As a result, post-processing steps like in nearly any AM process chain are needed after the printing step to finish and adjust the surface as the customer or application require [1, 6]. The disadvantage of additional post-processing can be counterbalanced in particular if the post-processing can generate additional extra value, e.g. through additional functionality. One opportunity to create such an additional functionality is ultra-short pulsed laser structuring. Ultra-short pulsed lasers were already used in studies according post-processing of additive manufactured metal surfaces with the aim to smoothen the surface [10 bis 12] or to correct form and contour deviations between the part as produced and the final geometry [13]. Sadly, the generated surfaces by direct laser ablation were still in the range of several microns, which makes them insufficient as optical surfaces.

Thus, this study investigated ultra-short puled laser ablation as additional part of the post-processing chain to create an additional surface functionality, e.g. optical gratings, on the additive manufactured parts.

2. Experimental setup

2.1. Sample preparation

For the conduction of laser ablation experiments a simple, cube geometry of the sample parts was chosen. The size of the cubes was 10 mm x 10 mm x 10 mm, so an assumed total test area of 7 mm x 7 mm could be realized without any problems and also no support structures were needed. Using the TRUMPF TruPrint100 Multilaser and a powder bed based additive manufacturing process allowed the production of 37 AlSi10Mg test cubes with a space of 2 mm between each cube to each side on a single built platform. As mentioned before, the surface of layer-wise printed objects is clearly too rough to use them directly for optical applications. Thus, different post-processing steps were carried out before the ablation experiments. These include a laser cleaning process to remove lose powder particles and oxide layers and a laser surface polishing process by surface remelting, see Fig. 1. As result the final samples for the ablation experiments exhibit a reduced surface roughness from $R_a = 9.78$ µm as built down to $R_a = 0.45$ µm. Additionally, a polished AlSi10Mg metal sheet with a surface roughness of $R_a = 0.1$ µm was structured with selected parameters for the optical diffraction experiments.

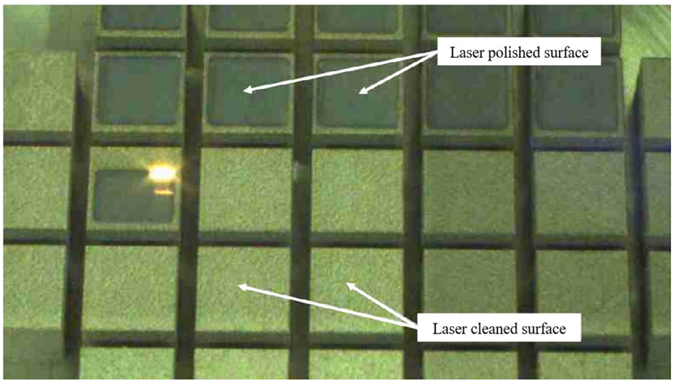

Fig. 1. Sample preparation. Laser polishing after laser cleaning.

2.2. Ultra-short pulsed laser ablation

The ablation experiments were performed on a microcut UKP workstation from LLT Applikations GmbH. This system is equipped with a Pharos PH1-20 system, Light Conversion, as ultra-short pulsed laser source and a galvo scanner system intelliSCAN III 14, SCANlab, including a F-Theta lens to guide the focused laser beam over the work piece. The synchronization between the laser source and the work station is realized using the remote control of the scanner controller as well as signal via the numeric control kernel of the microcut UKP station. Additionally, the machine is equipped with a camera-based measuring system for exact zero-point positioning and an exhaustion to remove ablation products and fume. Table 1 lists the used laser and program parameters for the conducted ablation test.

Table 1. Parameter settings for ablation experiments

Parameter	Unit	Value
Laser wavelength λ	nm	1030
Single pulse energy E_p	µJ	6.7 - 200
Pulse repetition rate f_{rep}	kHz	100; 200; 300
Scan velocity v_{scan}	m/s	0,5 – 2,5
Number of scans N_{Scan}	#	1 - 25
Pulse duration t_H	fs	800
Focal diameter d_f	µm	30
Line distance d_{hatch}	µm	1; 2; 10; 30; 40
Track overlap TO	%	97; 93; 67; 0; -33

2.3. Surface analytics

In the first stage, the structured surfaces were analyzed using white light interferometry with a NewVie8300, ZYGO. This allows a detailed measurement of the ablation depth and thus an accurate determination of the ablation threshold and the edge quality according burr formation.

To check the optical functionality a simple reflection test was performed for selected structuring parameters. These samples were irradiated with a broad band, tunable laser source in the visible wavelength range under a defined angle of incidence of 70°.

Afterwards, the diffraction pattern was measured on a detection screen a distance of 5.5 m.

3. Results

Fig. 2 shows the structured samples of the different process development steps. On the right side, 37 cubes with line patterns resulting from a first parameter study can be seen. The samples in the middle and on the left side show larger structures fields of 10 mm x 10 mm with promising parameters out of the parameter study.

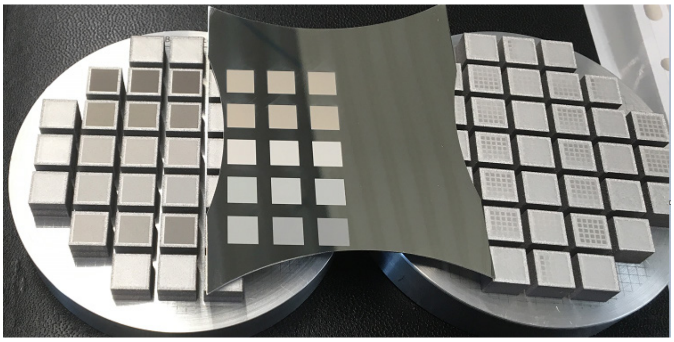

Fig. 2. Structured samples. Parameter study for the determination of possible process parameters (right), AM test samples for diffraction tests (left), structured reference sheet metal (middle).

3.1. Investigation of the ablation depth and threshold fluence

The ablation threshold fluence in this work is determined by the logarithmic dependency of the ablation depth z_{abl}, the applied peak fluence F and the threshold fluence F_{th}, see Eq. 1. Thereby, the peak fluence is calculated for a Gaussian beam and thus equals two times the adjusted single pulse energy E_p divided by the irradiated area or here focal area, respectively.

$$z_{abl} = \delta \ln\left(\frac{F}{F_{th}}\right) \quad (1)$$

A typical result of the ablation experiments according the ablation depth in relation to the used pulse repetition rate and fluence is displayed in Fig. 3 for a fix number of scans $N_{scans} = 10$ and scan velocity $v_{scan} = 1.5$ m/s.

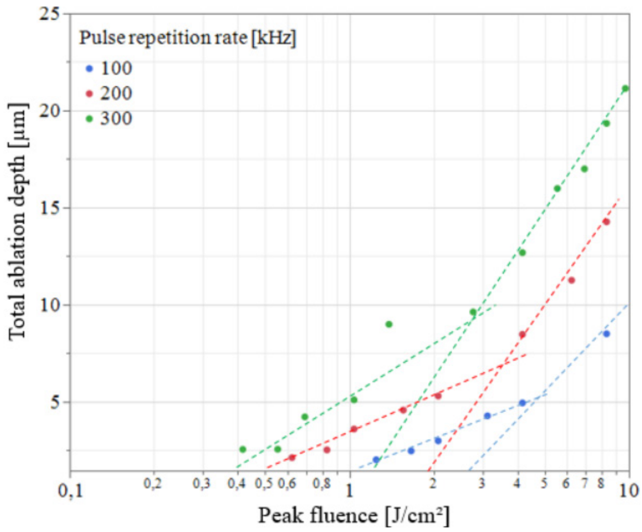

Fig. 3. Total ablation depth after 10 scans and a constant $v_{scan} = 1.5$ m/s, $f_{rep,1} = 100$ kHz (blue), $f_{rep,2} = 200$ kHz (red) and $f_{rep,3} = 300$ kHz (green).

Clearly, two common ablation regimes can be seen for all investigated pulse repetition rates. The first one is dominated by the optical properties of the material, the second one by its thermal properties. Additionally, higher repetition rates lead to a lower threshold fluence in the first regime and also a stronger increase of the ablation depth for higher fluence. This is mainly due to incubation and further heat accumulation.

The incubation effect and describes the correlation between the applied number of pulses per irradiated area and the single pulse threshold fluence by the following Eq. 2.

$$F_{th}(N) = F_{th}(1)N^{S-1} \quad (2)$$

Since incubation in this case is more dominant then heat accumulation, the single pulse threshold fluences for the additive manufactured test cubes are calculated using Eq. 2 and listed in Table 2.

Table 2. Determined threshold fluences for additive manufactured AlSi10Mg at a pulse duration of $t_H = 800$ fs, $\lambda = 1030$ nm and S = 0.8

Pulse repetition rate [kHz]	Threshold fluence [J/cm²]
100	1.14
200	0.65
300	0.57

For the fabrication of diffraction samples the final parameters were set to $f_{rep} = 300$ kHz, F = 1.04 J/cm², $v_{scan} = 1.5$ m/s and Nscan = 8, resulting in an ablation depth of approx. $z_{abl} = 2$ µm. This also results in a small width of the structures so features below the focal diameter $d_f = 30$ µm should generate a diffraction pattern.

3.2. Determination of the grating constant from resulting diffraction pattern

The experiments conducted with the laser polished samples showed no significant diffraction pattern and just scattered the light in various directions because of the high surface roughness. In contract, the structured surfaces on the polished metal sheet showed a clear diffraction pattern, see Fig. 4.

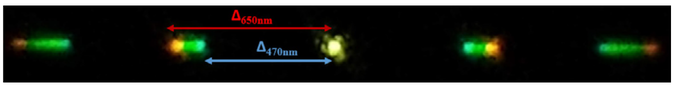

Fig. 4. Diffraction pattern of a sample-flied, structured with a line distance $d_{hatch} = 40$ µm, illuminated with the wavelength range $\lambda = 470$ nm – 650 nm.

For an accurate measurement of the distance between two diffraction maxima, the samples were only irradiated with one adjusted wavelength at a time. Table 3 lists the results of these measures. It can be seen that for lower line distances the distance between two maxima increases. Further it can be observed, that even for a line spacing of just 10 µm a diffraction pattern occurs, although this line distance is significant smaller than the used focal diameter $d_f = 30$ µm.

Table 3. Measured distance between two intensity maxima using different irradiation wavelengths

Line distance d_{hatch}	λ_1 = 470 nm	λ_2 = 550 nm	λ_3 = 650 nm
1 µm	-	-	-
2 µm	-	-	-
10 µm	-	310 mm	364 mm
30 µm	88 mm	102.5 mm	120.5 mm
40 µm	66 mm	76.5 mm	91 mm

With the results listed in Table 3 and Eq. 3, which is the lattice equation, it is possible to calculate the grating constant g and the real line distance, respectively. Here, k is the k-th maxima and d_k the distance from the zero order to the k-th order. Table 4 compares the theoretical results of d_{hatch} with the one calculated backwards from the diffraction pattern. They fit very well to each other only with slight deviations.

$$\lambda = \frac{g d_k}{km} \ and \ g = \frac{1}{d_{hatch}} \tag{3}$$

Table 4 Comparison of the adjusted line distance and resulted line distance from backwards calculation

	λ_1 = 470 nm	λ_2 = 550 nm	λ_3 = 650 nm
$d_{hatch, theo}$	$d_{hatch, real}$	$d_{hatch, real}$	$d_{hatch, real}$
10 µm	-	9.79 µm	9.86 µm
30 µm	29.48 µm	29.62 µm	29.78 µm
40 µm	39.31 µm	39.68 µm	39.43 µm

Further, it can be observed in Fig. 4, that the intensity of the maxima strongly decreases from the first to the second. This indicates still existing, undesirable scattering.

4. Discussion

The determined threshold fluences for ultra-short pulsed laser ablation of AM AlSi10Mg are close to values reported for pure aluminum in other work, e.g. F_{th} = 0.9±0.25 J/cm² [14]. Even a lower threshold value was achieved for higher repetitions rates, which indicates an influence of heat accumulation even for repetitions rates of just a few hundred kilohertz.

For the process of direct laser writing of optical gratings, the tested laser polishing process was an insufficient pre-treatment step, although the roughness was strongly deceased compared to its initial state. It seems that beside a low roughness also a glossy surface is required. Then, the experimental results fit very well with the theoretical approach, which could be demonstrated on a polished AlSi10Mg sheet.

5. Conclusion and outlook

Additive manufactured of AlSi10Mg might be a good solution to create optical reflectors. In general, it is possible to create surfaces with an optical functionality by direct laser writing using ultra-short laser pulses even with focal diameters of a few tens of microns. A clear diffraction pattern can be observed, if the distance between the surface and the screen is large enough and the initial surface quality is sufficient. Thus, future work will investigate the needed initial surface state for a good reflection result after a laser based post-processing chain. Further, smaller focal diameter to increase the diffraction capability of the surface by smaller feature sizes will be investigated.

Acknowledgements

The authors would like to thank Prof. Dr. Andreas Heinrich from the Center of Optical Technologies at Aalen University, for his support. We acknowledge support by the German Federal Ministry of Education and Research, program 'FH-Impuls' (Smart-ADD, grant no. 13FH4I06IA).

References

[1] Eyers, D. R. u. Potter, A. T.: Industrial Additive Manufacturing: A manufacturing systems perspective. Comput. Ind. 92-93 (2017), S. 208–218
[2] Schneck, M., Gollnau, M., Lutter-Günther, M., Haller, B., Schlick, G., Lakomiec, M. u. Reinhart, G.: Evaluating the Use of Additive Manufacturing in Industry Applications. Proc. CIRP 81 (2019), S. 19–23
[3] Heinrich, A. u. Rank, M.: 3D Printing of Optics. Bellingham: SPIE Press 2018
[4] Niesler, F. u. Tanguy, Y.: 3D Printers for the Fabrication of Micro-Optical Elements. Optik & Photonik 11 (2016) 4, S. 44–47
[5] Gissibl, T., Thiele, S., Herkommer, A. u. Giessen, H.: Sub-micrometre accurate free-form optics by three-dimensional printing on single-mode fibres. Nat. Commun. 7 (2016), S. 11763
[6] Heinrich, A., Börret, R., Merkel, M. u. Riegel, H.: Additive manufacturing of reflective and transmissive optics: potential and new solutions for optical systems. Proc. SPIE Vol. 10523 (2018), S. 1052302
[7] Lightweight structures for metal mirrors. Dimensional Accuracy and Surface Finish in Additive Manufacturing, Heidler, N., Hilpert, E., Hartung, J. u. Albert, T., Leuven 2017
[8] Bennett, H. E., Bennett, J. M. u. Ashley, E. J.: Infrared Reflectance of Evaporated Aluminum Films. J. Opt. Soc. Am. 52 (1962) 11, S. 1245
[9] Hass, G. u. Waylonis, J. E.: Optical Constants and Reflectance and Transmittance of Evaporated Aluminum in the Visible and Ultraviolet*. J. Opt. Soc. Am. 51 (1961) 7, S. 719
[10] Mingareev, I., Gehlich, N., Bonhoff, T., Meiners, W., Kelbassa, I., Biermann, T. u. Richardson, M. C.: Post-processing of 3D-printed parts using femtosecond and picosecond laser radiation. Proc. SPIE Vol. 8970 (2014), 89700R
[11] Worts, N., Jones, J. u. Squier, J.: Surface structure modification of additively manufactured titanium components via femtosecond laser micromachining. Opt. Commun. 430 (2019), S. 352–357
[12] Mingareev, I., Bonhoff, T., El-Sherif, A. F., Meiners, W., Kelbassa, I., Biermann, T. u. Richardson, M.: Femtosecond laser post-processing of metal parts produced by laser additive manufacturing. J. Laser Appl. 25 (2013) 5, S. 52009
[13] Holder, D., Leis, A., Buser, M., Weber, R. u. Graf, T.: High-quality net shape geometries from additively manufactured parts using closed-loop controlled ablation with ultrashort laser pulses. Adv. Opt. Technol. 9 (2020) 1-2, S. 101–110
[14] Zayarny, D. A., Ionin, A. A., Kudryashov, S. I., Makarov, S. V., Kuchmizhak, A. A., Vitrik, O. B. u. Kulchin, Y. N.: Surface ablation of aluminum and silicon by ultrashort laser pulses of variable width. Jetp Lett. 103 (2016) 12, S. 752–755